geosciences

MDPI

Article

Sulfur, Strontium, Carbon, and Oxygen Isotopes of Calcium Sulfate Deposits in Late Carboniferous Rocks of the Loei-Wang Saphung (LWS) Area, Loei Province, Thailand

Nusara Surakotra [1,*], Sarunya Promkotra [1], Punya Charusiri [2], Teruyuki Maruoka [3] and Ken-inchiro Hisada [3]

1 Department of Geotechnology, Faculty of Technology, Khon Kaen University, Khon Kaen 40002, Thailand; sarunya@kku.ac.th
2 Department of Geology, Faculty of Science, Chulalongkorn University, Bangkok 10330, Thailand; Punya.C@chula.ac.th
3 Graduate School of Life and Environmental Sciences, University of Tsukuba, Ibaraki, Tsukuba 305-8572, Japan; maruoka.teruyuki.fu@u.tsukuba.ac.jp (T.M.); hisadak@geol.tsukuba.ac.jp (K.-i.H.)
* Correspondence: nussan@kku.ac.th; Tel.: +66-891-345-890

Received: 30 May 2018; Accepted: 20 June 2018; Published: 22 June 2018

Abstract: Sulfate deposits of the Loei-Wang Saphung (LWS) area, northeastern Thailand, intercalated with carbonate and silicic clastic rock were analyzed for S, O, C, and Sr to determine the depositional environment, as well as the age of formation. Sulfate samples yielded average values of $\delta^{34}S$ of 14.6‰, while the $^{87}Sr/^{86}Sr$ ratio of gypsum was 0.708282 and that of anhydrite was 0.708288. The carbonate layers yielded average $\delta^{18}O_{PDB}$, and $\delta^{13}C$ values of −12.5‰ and −0.1‰, respectively. Our results revealed that the LWS evaporite deposits were originally formed from seawater, and the relatively negative value of $\delta^{18}O$ was a result of meteoric alteration during subaerial exposure of the sections. Comparing these isotopic values with the nearby Nakon Sawan sulfate deposits, the Sr isotopes showed slightly higher values with very mild variations. These isotopic values suggest that the LWS deposits were not affected by subsequent hydrothermal alteration by younger igneous dikes in this area. Therefore, some of these isotope signatures are considered to be primary features of the deposit, despite the fact that the deposit underwent anchizone to epizone metamorphism. The S and Sr isotope values support the depositional age of the LWS sulfate deposit in the Middle to Late Carboniferous.

Keywords: Loei-Wang Saphung (LWS); calcium sulfate deposits; stable isotope

1. Introduction

Evaporites are highly susceptible to diagenesis, which significantly affects rock structures, mineralogy, and fabrics [1]. The "diagenetic sulfate cycle" consists of the transformation of gypsum to anhydrite due to progressive burial or the transformation of anhydrite to gypsum due to surface exposure from uplifting [2]. This change can lead to a partial or complete obliteration of the original structure of rocks due to the difference in volume and density of both minerals involved. An isotope study may help to determine the environment of deposition and stages of alterations, as well as the diagenetic factors controlling alteration.

Gypsum–anhydrite deposits are present in many parts of Thailand. They can be grouped into three categories based upon their lithology and age association, including (1) deposits associated with Pre-Mesozoic rocks; (2) deposits associated with Mesozoic rocks; and (3) deposits associated with Post-Mesozoic rocks. The Loei-Wang Saphung area (LWS), northeastern Thailand (Figure 1)

contains a deposit associated with Pre-Mesozoic rocks, which is similar to the Nakon Sawan area in central Thailand.

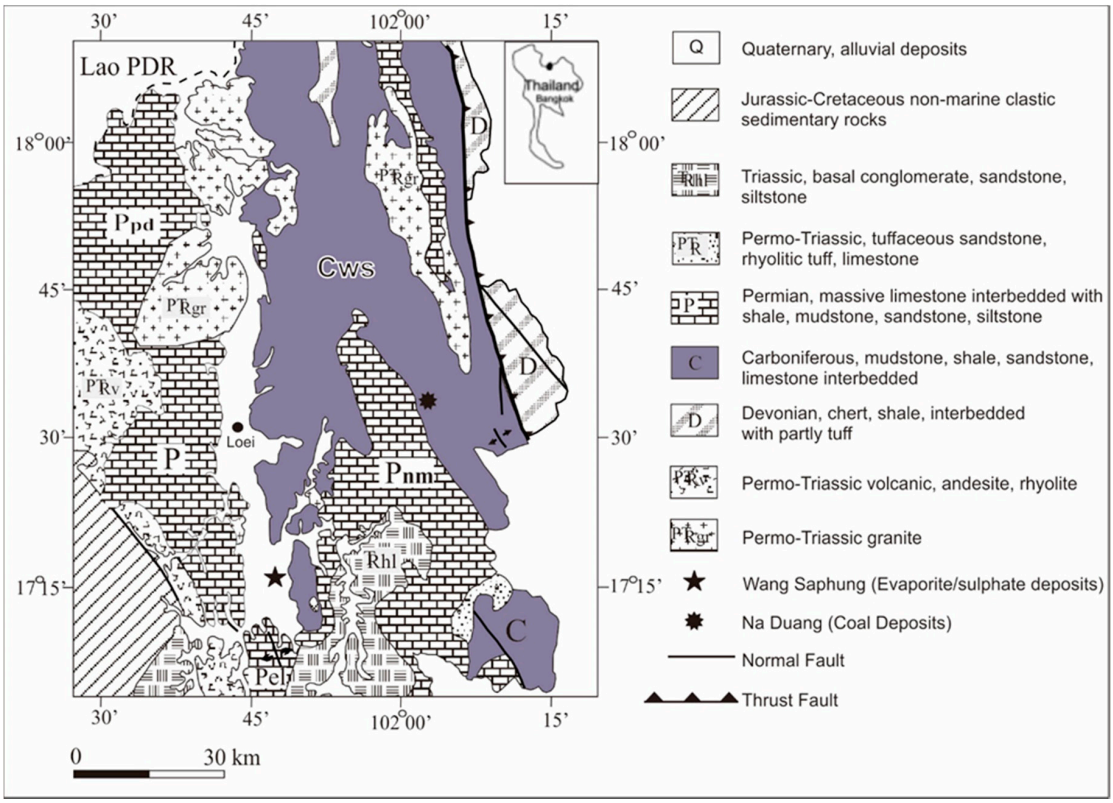

Figure 1. Geological map showing the locations of the Loei-Wang Saphung area (LWS) evaporate/sulfate deposits in the Loei Province, northeastern Thailand (modified after Department of Mineral Resources of Thailand (DMR), 2005) [3].

The LWS deposits are present below the surface as sulfate laminae alternating with carbonate and siliciclastic rocks. Lithologic studies of the LWS sulfate deposits were published by Utha-aroon et al. (1996) [4] and Surakotra et al. (2017) [5]. These deposits lie in an important location for the potential documentation of tectonic events, such as the closing of the Tethys seaway during the Late Paleozoic. The deposits also provide evidence of climatic events, such as the warm and moist conditions during the Early to Mid-Carboniferous, which are indicated by the coal deposits [6,7] and the dry and arid conditions during the Middle to Late-Carboniferous, which are indicated by evaporite sulfate deposits [5]. As shown in Figure 1, two contrasting depositional environments can be recognized in the Carboniferous Wang Saphung (CWS) unit, one in the northeast where the Na Duang coal deposit is located and the other in the southwest where the evaporite deposit is located. Laveine et al. (2003, 2009) [6,7] studied the coal deposits in detail and reported that the abundant plant fossils found within represented a non-marine environment in the Visean (Early Carboniferous) age.

The geology of gypsum–anhydrite deposits still requires verification and further refinements. A preliminarily macroscopic observation on the depositional and post-depositional features of the gypsum deposits by Utha-aroon et al. (1995) [4] suggested a secondary transformation from a hypersaline lagoon that was the result of a brief marine transgression and subsequently evaporated into Tertiary grabens. An investigation by Fontaine et al. (1997) [8] on microfossils in limestone associated with a gypsum deposit in this area suggested that the deposit was of marine origin during the Late-Carboniferous (Moscovian). Surakotra et al. (2017) [5] also reported evidence of marine fossils in carbonate beds within this area, suggesting a Moscovian age. Hence, the age and origin of the deposits are still considered preliminary and require further investigation. In this regard, Sr, S, C,

and O isotope studies are particularly useful in monitoring the age and depositional environment as (1) some of the isotope ratios in seawater are constant at any point in time (within the limits of analytical precision), (2) these isotope ratios have varied in time in well-constrained manners [9–11], and (3) the $^{87}Sr/^{86}Sr$ and $\delta^{34}S$ values of seawater are generally distinct from that of river water [12,13].

Although these sulfates are commonly thought to be completely altered and that it is impossible to determine the specific composition and temperature of the solution at the time the gypsum was precipitated, many depositional and diagenetic structures and geochemical data have survived in these sulfate rocks. Even though the evaporite deposits in this area are not economic, they are important for the geological aspect, as they are an essential key in interpreting the paleogeography and paleoclimate during the time of deposition. A detailed study on the petrology and alteration of the LWS deposits is presented in a previous work by Surakotra et al. (2017) [5]. The objective of this paper was to examine the evidence regarding the geochemical data of the LWS sulfate deposits in order to trace the diagenetic alterations and help interpret the age and depositional environment of its formation.

2. Materials and Methods

2.1. Geology of the LWS Area

The Loei and Petchabun fold belts were formed in response to convergent tectonics of the Shan-Thai and the Indochina terranes during the closure of the Paleo-Tethys Ocean by the end of the Permian to Early Triassic [14–16]. The LWS study area is located near the northwestern edge of the Khorat Plateau (Indochina terrane). The oldest rocks are low-grade metasedimentary rocks of Devonian age, cropping out in the eastern part of the Loei area. The rocks are alternated with volcanic clastic rocks and overlain by the more widespread carboniferous marine sedimentary rocks in the middle part. The Devonian strata are in contact with the overlying rocks by a thrust fault [17]. The younger sedimentary rocks are Permian marine strata, continental Mesozoic rocks (the Mesozoic Khorat Group), and recent sediments. The names and stratigraphic relationships of the rocks in the Loei and the adjacent area are shown in Figure 1.

The study area presents carboniferous marine sediment belonging to the CWS Formation in Figure 1. The area lies in a narrow valley of the Loei River in the Wang Saphung District, about 20 km south of the Loei Province, which is a part of a graben structure running roughly in a north-south direction. It is a small evaporite deposit with up to 50 m thick gypsum–anhydrite beds. The evaporite deposits are overlain by cross-laminated and fine-grained siliciclastic and carbonate rocks of the Carboniferous to Permian ages. A detailed petrological and alteration account of the sulfate and interbedded rocks, as well as general stratigraphic information, is given in Surakotra et al. (2017) [5].

As documented in Surakotra et al. (2017) [5], the limestones are dominated by calcimudstone, peloidal wackstone or packstone, algal boundstone, and fenestral carbonate mudstone with only local evidence of cementation or replacement. These beds suggest a shallow marine deposition, that was accumulated in a tidal flat to subtidal environment. The sulfate petrography can be classified into 10 textures viz. alabastrine gypsum, satin spar gypsum, selenite gypsum, gypsarenite, porphyroblastic gypsum, fine lenticular gypsum, crystalloblastic or blocky anhydrite, prismatic anhydrite, epigenetic anhydrite, and felty epigenetic anhydrite. The results indicate that the LWS sulfate deposit has passed through at least four stages of alteration.

2.2. Sample Collecting and Analysis

The succession of gypsum–anhydrite deposits is studied from core rocks. The sedimentary texture and lithology of gypsum, anhydrite, and related rocks were examined from logged cores of 30 exploration wells in the Loei-Wang Saphung area (total depth of 1799 m), archived by the Department of Mineral Resources of Thailand (DMR). The rock slabs made from rock samples collected from the exploration cores were examined for the texture and composition of gypsum, anhydrite, and related rocks. A total of 180 thin sections were prepared from gypsum, anhydrite, and other

related rocks from the boreholes and mines for petrographic analysis and examined for their diagenetic evolution [5].

A total of 50 samples of carbonate laminae and clasts within the gypsum–anhydrite beds and associated carbonate rocks in the exploration wells and one sample of pyrite crystals from the carbonate clasts in the gypsum bed of the Wang Saphung area were removed with a dental drill and analyzed for their carbon and oxygen isotope ratios at Monash University using a Finnigan MAT 252 mass spectrometer. CO_2 from the carbonate was liberated by acidification using H_3PO_4 in a He atmosphere at 72 °C in a Finnigan MAT GasBench and analyzed by continuous flow. The results were normalized at the same time using both the International Atomic Energy Agency (IAEA) standard CO-1 and the internal laboratory standards. The isotopic values were expressed in standard δ notation relative to PDB (Pee Dee Belemnite) for oxygen and V-PDB (Vienna Pee Dee Belemnite) for carbon. Many samples were analyzed twice, and the precision (1sd) based on replicate analyses was $\delta^{18}O = \pm 0.1‰$; $\delta^{13}C = \pm 0.1‰$.

A total of nine powdered samples of sulfate rocks were analyzed for concentrations and compositions of the sulfur isotope using an elemental analyzer/isotope-ratio mass spectrometer (EA/IRMS) system (Isoprime-EA, Isoprime) at the University of Tsukuba. The analytical procedures and conditions were described by Maruoka et al. (2003) [18]. The sulfur isotopic compositions were expressed in terms of $\delta^{34}S$ (‰) relative to the Vienna Canyon Diablo Troilite (V-CDT) standard and were determined with a precision of ±0.2‰ (1σ). Two standard reference materials for sulfur (IAEA-S-1 and -2) were used for calibrating the sulfur contents and for correcting the instrumental mass discrimination of the IRMS.

Four selective gypsum and anhydrite samples were analyzed for the strontium isotope at the Japan Agency for Marine-Earth Science and Technology (JAMSTEC) using a method described by Roveri et al. (2014) [19], with slight modifications. Sr was separated using the Eichrom Sr Spec resin. Matrix elements were eluted in 6 M HNO_3 and 3 M HNO_3 before collecting Sr with 0.05 M HNO_3. The total procedural blank for the Sr samples prepared using this method was less than 10 pg. Samples were loaded onto single Re filaments with a Ta-activator [20], and the Sr isotopic composition of each sample was measured with a Thermo Scientific TRITON TI thermal ionizing mass spectrometer at JAMSTEC. The data were acquired in static multi-collection mode and computed from 10 blocks of 15 cycles with an integration time of 15 s for each cycle. The $^{87}Sr/^{86}Sr$ ratio was normalized for mass fractionation using an exponential law correction to the $^{87}Sr/^{86}Sr$ ratio of 0.1194. Analytical accuracy was evaluated by measuring NIST SRM 987, which provided readings of 0.7102455 ± 0.0000011 (2 S.D., $n = 3$) during the course of this study. The Sr isotope measurements were performed with an ^{88}Sr ion beam intensity of 3–5 V.

3. Results

3.1. $\delta^{34}S$ Values

Gypsum and anhydrite from the drill-hole of the LWS area were selected for sulfur and strontium isotope analysis. Gypsum samples were mainly microcrystalline gypsum with minor amounts of granular xenotopic gypsum and prismatic idiotopic gypsum. The alabaster gypsum and gypsum grains that have been deformed by ductile flow textures suggest that the gypsum originated through the hydration of former anhydrite [5]. Anhydrite samples consisting of densely packed, elongated anhydrite laths, crystalloblastic or blocky anhydrite, and felty epigenetic anhydrite texture indicate that they resulted from the dehydration of the former gypsum.

Stable isotope measurements were analyzed from nine samples of sulfate of the LWS deposits, which consisted of five samples of gypsum and four samples of anhydrite. The $\delta^{34}S$ values of the gypsum varied from 14.5 to 15.5‰, with an average of 15.0‰. The $\delta^{34}S$ values of the anhydrite varied from 14.0 to 14.6‰, with an average of 14.3‰. In addition, the average $\delta^{34}S$ of both gypsum and anhydrite was 14.6‰.

The $\delta^{34}S$ values of both gypsum and anhydrite varied in a narrow range from 14.0 to 15.5‰. The similar values of $\delta^{34}S$ in both the gypsum and anhydrite indicated that the deposit was homogeneous. The different lithofacies could have been affected by the burial diagenesis of sulfate rocks in such a way that the gypsum transformed to anhydrite by the dehydration process at depth, and anhydrite rehydrated to gypsum during uplift. The sulfur isotopic compositions of the LWS area are slightly lower than the Nakon Sawan sulfate deposits, as described by Kuroda et al. (2016) [21]. The $\delta^{34}S$ values of our gypsum samples fit well with the ocean water sulfate $\delta^{34}S$ curves between the Early to Middle Carboniferous and between the Late Triassic and younger ages (Figure 2).

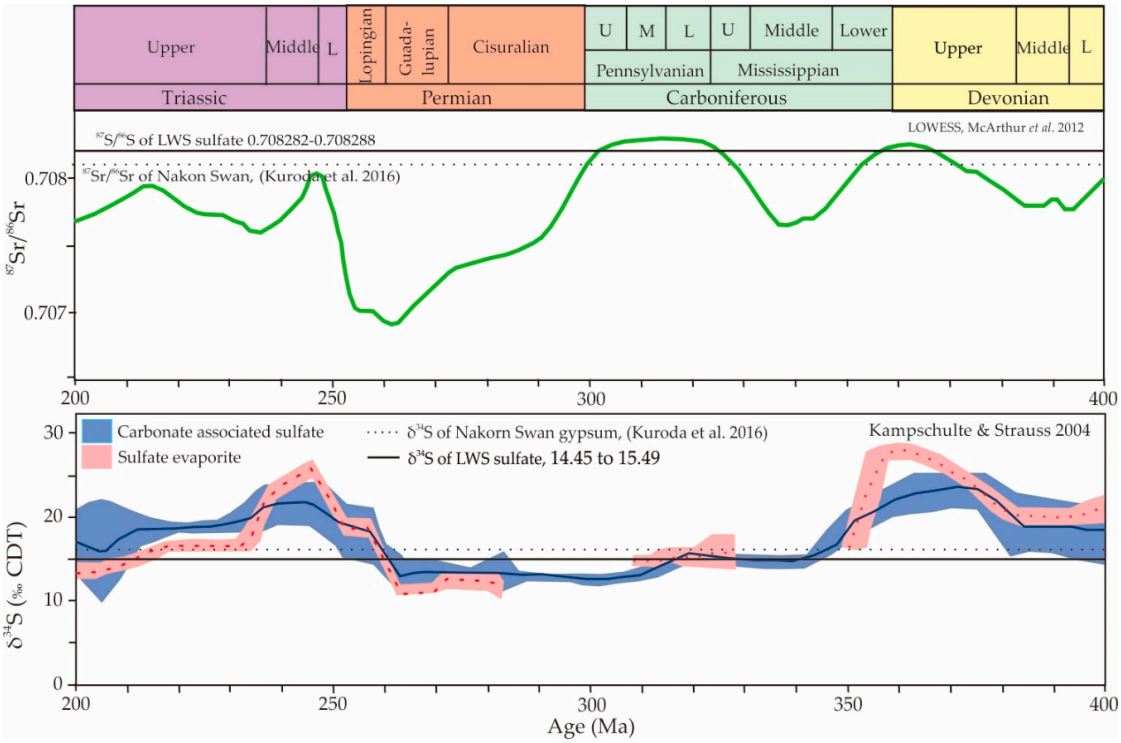

Figure 2. Secular variations of strontium ($^{87}Sr/^{86}Sr$, **middle** panel) and sulfate sulfur ($\delta^{34}S$, **bottom** panel) isotopic compositions in ocean water from 400 to 200 Ma. The $^{87}Sr/^{86}Sr$ values (green curve) are from Locally Weighted Scatterplot Smoothing (LOWESS) (data compiled by McArthur et al. 2012 [22]), and the $\delta^{34}S$ values of carbonate-associated sulfates (blue curve) and sulfate evaporites (red) were compiled by Kampschulte and Strauss (2004) [23]. Horizontal lines indicate the data for the LWS sulfate samples when compared with the Nakon Sawan gypsum samples analyzed by Kuroda et al. (2016) [21].

3.2. Strontium Isotope

Four samples of sulfate minerals were analyzed for $^{87}Sr/^{86}Sr$ ratios, but two samples failed during the analysis. One was the alabastrine gypsum lithofacies, which gave a $^{87}Sr/^{86}Sr$ ratio of 0.708282. The other was anhydrite, which had a $^{87}Sr/^{86}Sr$ ratio of 0.708288. The values of the sulfur and strontium isotopes and the information of the samples are shown in Table 1. The values almost fit with the highest peaks during the Late Paleozoic times of the standard curve (Figure 2), one was around the D-C boundary and the other was in the Middle Pennsylvanian Period (around Bashkirian–Moscovian). The latter case also fit well with the stratigraphic data, where the gypsum beds were apparently overlain by limestone with late Moscovian marine fossils from previous works [5,8]. We compared our results to the Nakon Sawan sulfate deposits [21], which are also associated with Carboniferous rock similar to the LWS deposits. Our results were slightly higher than the values of the Nakon Sawan deposits.

Table 1. Stable sulfur and strontium isotope ratios of the gypsum–anhydrite beds in the exploration wells, Wang Saphung area, Loei Province, Thailand.

Sample	Drill Hole No.	Depth (m)	δ^{34}Scalc (‰)	$^{87}Sr/^{86}S$	Comments
NS-1-anh	WP03	73.0	14.1		Near volcanic contact
NS-2-anh	WP03	79.5	14.0	0.708288	Dense anhydrite
NS-4-anh	WP10	23.5	14.4		Dense anhydrite
NS-6-anh	WP28	64.5	14.6		Dense anhydrite
Average			14.3		
SD			00.3		
NS-3-gyp	WP04	27.0	15.0	0.708282	Alabastrine gypsum
NS-5-gyp	WP20	67.3	15.5		Selenite gypsum
NS-7-gyp	WP29	32.0	14.5		Alabastrine gypsum
NS-9-gyp	WP30	36.8	14.6		Alabastrine gypsum
NS-10-gyp	WP30	52.5	15.3		Alabastrine gypsum
Average			15.0		
SD			00.4		

3.3. Carbon Isotope

Stable isotopes were measured from 50 samples of carbonate from the LWS sulfate deposits, which consisted of 14 samples of the micritic-limestone laminae and micritic-limestone clast within the gypsum–anhydrite beds and 36 samples of associated carbonate rocks in the exploration wells.

The $\delta^{13}C$ values of the carbonate samples varied from −5.9‰ to 4.8‰ with an average of −0.4‰, and the standard deviation from the average $\delta^{13}C$ value was +3.4‰. The $\delta^{13}C$ values of the micritic-limestone laminae and micritic-limestone clast within the gypsum-anhydrite beds varied from −5.8‰ to 3.5‰ with an average of −2.4‰, and the standard deviation from the average $\delta^{13}C$ value was +3.2‰.

3.4. Oxygen Isotope

Stable isotopes were measured from the same samples of carbonate from the LWS sulfate deposits that were analyzed for carbon isotopes.

The $\delta^{18}O$ (PDB) values of the carbonate samples varied from −16.6‰ to −5.5‰ with an average of −12.5‰, and the standard deviation from the average $\delta^{18}O$ value was +3.5‰. The $\delta^{18}O$ (PDB) values of the micritic-limestone laminae and micritic-limestone clast within the gypsum–anhydrite beds varied from −15.5‰ to −12.1‰ with an average of −14.0‰, and the standard deviation from the average $\delta^{18}O$ value was +1.3‰. The negative oxygen isotope could be related to meteoric water, high temperature alteration with marine water or groundwater, or alteration with hydrothermal fluids.

As reported in Surakotra et al. (2017) [5], the geometry of these sulfate deposits showed a karst topography at depth. The karstification of sulfate is the result of the solution process under different hydrodynamic behaviors of gypsum. Supporting evidence of weathering and erosion are the breccia clast of the associated rocks at the contact top of the gypsum body. Hence, the negative oxygen isotope in this area could have been an effect of meteoric alteration during subaerial exposure. Stable carbon and oxygen isotope values of carbonate laminae and clasts within the gypsum–anhydrite beds and associated carbonate rocks are shown in Table 2.

The cross-plots of the C and O isotopes for all samples showed a wide distribution of data, while the $\delta^{18}O$ and $\delta^{13}C$ cross-plots of the carbonate laminae and clasts within the gypsum–anhydrite beds showed a tendency to negative values. The cross-plots of carbon with oxygen isotopes are useful in determining the origin of evaporitic carbonate [2]. When we compared our cross-plots with the Nammal Formation along the different carbonate rocks proposed by Hudson (1977) [21] (Figure 3), the LWS carbonate rocks fell into the area of common marine limestone.

Table 2. Stable carbon and oxygen isotope values of carbonate laminae and clasts within the gypsum–anhydrite beds and associated carbonate rocks from the exploration wells, Wang Saphung area, Loei Province, Thailand.

Sample	Drill Hole No.	Depth (m)	^{13}C	$^{18}O_{PDB}$	Comments
AA1	WP2	54.26	4.1	−11.4	Micrite
AA1	WP2	54.26	4.3	−11.8	Duplicate run
AA2	WP2	54.26	4.4	−9.1	Crystalline (grainier)
AA21	WP2	41.20	4.5	−11.6	Limestone
AA54	WP3a	47.00	1.9	−15.3	Micritic limestone
AA56	WP3a	40.30	1.8	−15.2	Micrite limestone
AA55	WP3b	47.00	2.2	−15.9	Fractured coconut calcite
N2	WP4	16.60	1.0	−9.1	Calcite (recrystallized)
AA17	WP6a	18.30	0.5	−15.0	Limestone
AA5	WP7b	38.00	4.5	−10.7	Crystalline (grainier)
N5	WP9	40.00	2.3	−11.1	Fossil
AA35	WP9a	48.00	3.0	−14.9	Grey limestone
AA36	WP9b	48.00	1.3	−14.3	Late-stage white vein fill carbonate
N6	WP12	36.50	–5.4	−15.0	Sparite
N7	WP12	36.50	–2.7	−16.6	Calcite vein
AA32	WP13c	37.20	4.8	−5.5	Crackle breccia matrix
AA40	WP15	11.00	–1.3	−11.1	Limestone
N8	WP16	16.60	1.2	−10.9	Carbonate within sandstone
N9	WP16	16.60	0.3	−10.3	Carbonate within sandstone
AA27	WP17b	39.50	3.7	−8.5	Crystalline grainy limestone
AA29	WP17b	23.70	2.7	−10.1	Crystalline (grainier)
AA24	WP23a	82.30	3.1	−12.5	Limestone
N10	WP30	32.00	3.5	−12.8	Calcite (grind)
N12	WP30	32.00	3.0	−12.8	Calcite (recrystallized)
N17	WP30	39.70	–3.5	−12.4	Recrystallized carbonate
N1	WP4	16.6	–1.5	−9.1	Dolomite replaced by Fe-oxide material
AA26	WP17a	39.50	–1.9	−10.6	Buff dolomite clast
N11	WP30	32.00	3.5	−12.8	Dolomite
N3	WP4	16.60	–2.1	−9.2	Dark mineral on fracture
N13	WP30	39.70	–3.6	−12.8	Pyritic
AA4	WP7a	38.00	3.8	−14.8	Micrite
AA28	WP17a	23.70	1.9	−12.0	Micrite clast
AA49	WP30	36.80	–1.3	−14.7	Micrite clast
N14	WP30	39.70	–4.1	−12.1	Micrite lamina
N15	WP30	39.70	–3.0	−12.2	Micrite
AA11	WP30a	54.00	–4.6	−15.4	Micrite clast
AA47	WP30a	39.70	–3.8	−14.9	Micrite rim
AA13	WP30b	40.00	–4.0	−15.5	Micrite (radial textured)
AA15	WP30b	32.70	–4.3	−15.3	Micrite (unreplaced)
AA45	WP30b	60.50	–5.8	−15.2	Altered buff-green rim
AA46	WP30c	60.50	–5.8	−15.34	Light flow-contorted
Maximum			4.8	−5.5	
Minimum			–5.8	−16.6	
Average			–1.0	−12.5	

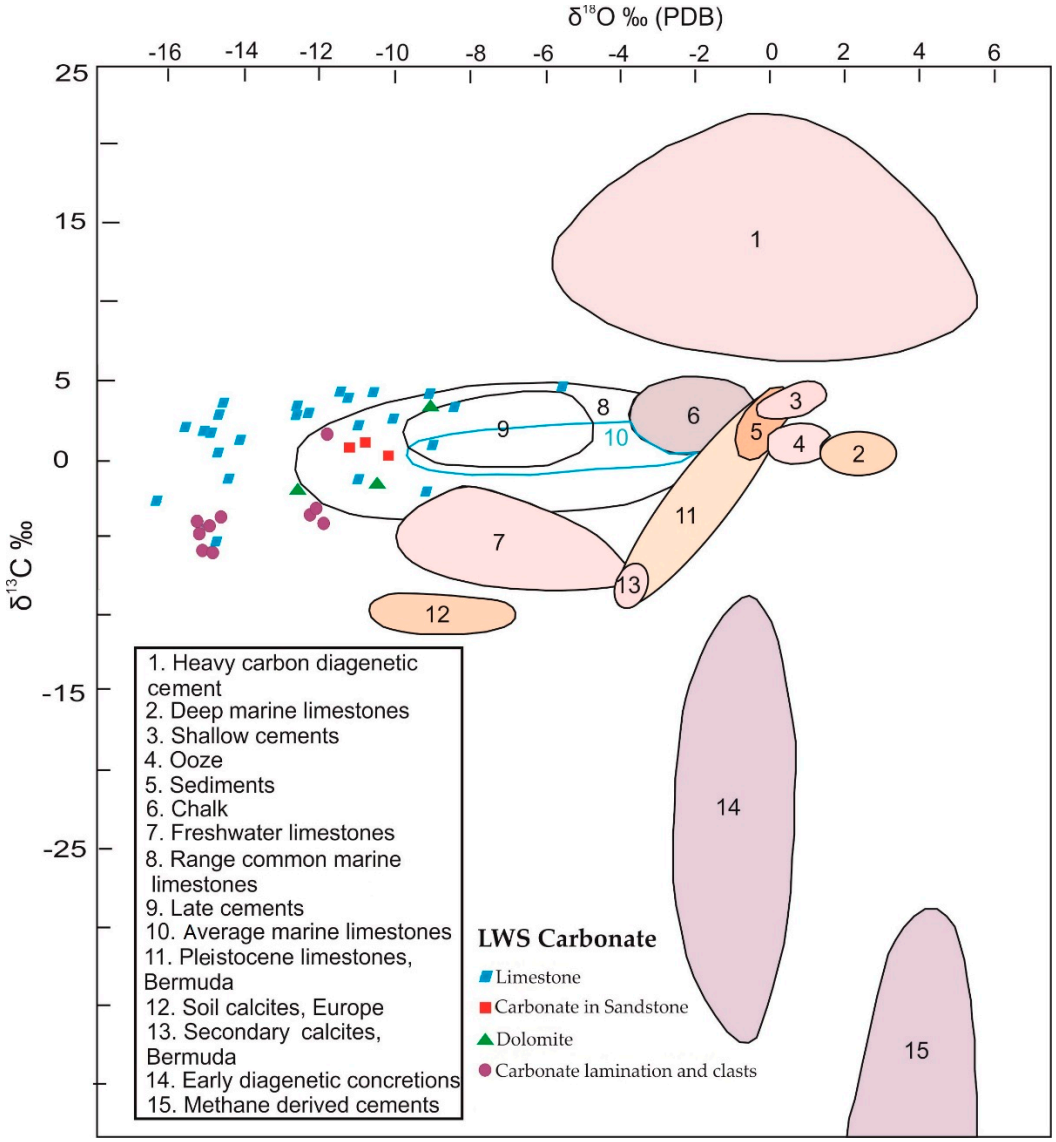

Figure 3. The $\delta^{18}O$ ‰ (PDB) and $\delta^{13}C$ ‰ cross-plots of carbonate laminae and clasts within the gypsum–anhydrite beds and associated carbonate rocks in the study area when compared with the carbonate rocks of the Nammal Formation proposed by Hudson (1977) [24].

4. Discussion

The LWS evaporites that stratigraphically underlie the Permian carbonate/clastic rocks are possibly older. However, we found that the evaporite layers were present, alternating with the limestones, as well as the clastic rocks, suggesting that both gypsum and carbonate/clastic rocks have been deposited with a lateral facies change condition. Since the age of carbonate rocks have been herein assigned as Middle Carboniferous by fossil assemblages [5,8], we interpreted that both evaporite and carbonate/clastic sequences were partly coeval and had formed in the same basin during the Middle Carboniferous. The lithological and mineralogical features of the LWS sulfate deposits were similar to those of the Nakhon Sawan area, as described by Kuroda et al. (2016) [21], who interpreted that the sulfate deposits of Nakhon Sawan were originally precipitated in a shallow marine environment on the floor of a lagoon or shelf.

The $\delta^{34}S$ value variations were largely resistant to isotopic fractionation during burial alteration and transformation [25]. Gypsum dehydration to anhydrite did not involve significant isotopic fractionation or a diagenetic redistribution of material in the subsurface. The LWS $\delta^{34}S$ values yielded

a narrow range between 14.0‰ and 15.3‰ for both gypsum and anhydrite. We interpreted the $\delta^{34}S$ values as primarily reflecting those of the co-existing seawater (brine), which meant that the $\delta^{34}S$ values of the gypsum were correlated to the $\delta^{34}S$ values of contemporaneous ocean water sulfates. The $^{87}Sr/^{86}Sr$ values of the gypsum and anhydrite samples fell in a very narrow range between 0.708282 and 0.708288. The strontium isotopic compositions of evaporitic sulfates are known to be identical to those of ocean water, provided that the brine (saline seawater) is fully connected with the ocean water.

Nevertheless, a comparison between the S and $^{87}Sr/^{86}S$ values' compositions of the marine evaporites with the values for contemporaneous seawater [22,26] revealed that most of the sulfate minerals analyzed from these deposits were simply derived from the precipitation of evaporated seawater.

We also compared our results with the Nakon Sawan sulfate deposits that were studied by Kuroda et al. (2017) [21], as the deposits had some similarity in age and the associated rocks. We found that both the S and $^{87}Sr/^{86}S$ values were slightly different. Therefore, the S and $^{87}Sr/^{86}S$ values revealed that both sites were formed from seawater. The difference of the results could be interpreted as these two sulfate deposits having occurred in quite dissimilar times of deposit and environments.

The slightly negative value of $\delta^{13}C$ in the micritic-limestone laminae and limestone clast within the gypsum–anhydrite beds suggested a contribution of light CO_2 in the carbonate system, either directly from atmospheric CO_2 fractionated in conditions of high photosynthetic demand [27] or from CO_2 derived from organic carbon oxidation.

Dickson and Coleman (2009) [28] pointed to the negative correlation of $\delta^{13}C_{carb}$ and $\delta^{18}O_{carb}$ values, where the isotopic signals were a result of meteoric alteration during subaerial exposure of the sections. While the meteoric-water diagenesis usually results in ^{18}O and ^{13}C depletions [29,30], such trends are also ubiquitous in modern diagenetically unaffected carbonates [31].

Together, the sedimentological and geochemical criteria indicate a hypersaline environment for the initial deposition of evaporative carbonate and subsequent early diagenetic alteration by a combination of meteoric and evaporated waters often associated with bacteria diagenesis [32].

The sulfur and oxygen isotopes indicated the age of the deposits through a comparison with the sulfur–oxygen age curve proposed by various authors [10,33]. Figure 2 shows a plot of the LWS data with the sulfur age curve [33], where it can be seen that our data fit well with the ocean water sulfate $\delta^{34}S$ curves of the Late-Carboniferous and between the Late Triassic and younger ages.

5. Conclusions

The results of the O, S, C, and Sr isotope investigations of the sulfate–carbonate deposits of the Loei-Wang Saphung (LWS) area together with previous geological syntheses led us to the following conclusions:

(1) Stable isotope data revealed that the LWS evaporite deposit was originally formed from seawater. The evidence was found in both S and Sr from the sulfate beds and C and O from the carbonate beds. Therefore, the evaporite and carbonate sequence must have been formed in the same basin during the same time.

(2) The negative value of the $\delta^{18}O$ isotopic signal was a result of meteoric alteration during subaerial exposures of the sections.

(3) The $\delta^{34}S$ values indicated an age of Late-Carboniferous and between the Late Triassic and Tertiary ages, while the Sr isotope indicated an age of Late Paleozoic during the Middle to Late Devonian and Middle to Late Carboniferous. Combined with the results of microfossils analysis from previous work [5,8], the age of these deposits is most likely the Middle to Late Carboniferous.

These isotope signatures are considered as the preserved primary depositional features, despite the fact that the deposit underwent anchizone to epizone metamorphism. The results of the S and Sr isotope values are supported by previous work, where the depositional age of the LWS sulfate deposit was in the Middle to Late Carboniferous. All lines of evidence suggest that the LWS sulfate

deposit is not unique and is similar, to some extent, to the Nakon Sawan sulfate deposit further in the south. These two sulfate deposits occurred in quite dissimilar times of deposit and environments. This suggests that the sulfate deposits occurred in the contrasting tectonic block to the area adjacent to the east either by the major fault or a tectonic line.

Author Contributions: N.S. was responsible for planning the research methodology, carrying out the research, analyzing the data, and concluding the research results. T.M. was responsible for laboratory test. S.P., P.C. and K.-i.H. supervised the research and reviewed the research manuscript.

Funding: This research was funded by the Japan Society for the Promotion of Science (JSPS).

Acknowledgments: The authors would like to acknowledge the Department of Primary Industries and Mines, Thailand, who provided the data for this research. The authors would like to show appreciation to Monash University, University of Tsukuba, and JAMSTEC for providing excellent cooperation and laboratory support during this research.

Conflicts of Interest: The authors declare no conflict of interest.

References

1. Kasprzyk, A. Gypsum-to-anhydrite transition in the Miocene of southern Poland. *J. Sediment. Res.* **1995**, *65*, 348–357.
2. Warren, J.K. *Evaporites: Sediments, Resources and Hydrocarbons*, 1st ed.; Springer: Berlin, Germany, 2006; p. 1036, ISBN 978-3-540-32344-0.
3. Department of Mineral Resources (DMR). *Geological Map of Loei Province (1:100,000)*; Department of Mineral Resources: Bangkok, Thailand, 2007.
4. Utha-aroon, C.; Surinkum, A. Gypsum exploration in Wang Saphung, Loei. In Proceedings of the International Conference on Geology, Geotechnology and Mineral Resources of Indochina (Geoindo 1995), Khon Kaen, Thailand, 22–25 November 1995; Youngme, W., Buaphan, C., Srisuk, K., Lertsirivorakul, R., Eds.; Department of Geotechnology, Khon Kaen University: Khon Kaen, Thailand, 1995; pp. 255–266.
5. Surakotra, N.; Charusiri, P.; Promkotra, S.; Hisada, K. Petrology and alteration of calcium sulfate deposits in Late Paleozoic rocks of Wang Saphung area, Loei Province, Thailand. *J. Earth Sci. Clim. Chang.* **2017**, *8*. [CrossRef]
6. Laveine, J.; Ratanasthien, B.; Sititach, S. The Carboniferous flora of Northeastern Thailand. *Rev. Palaeobiol. Geneve* **2003**, *22*, 761–797.
7. Laveine, J.; Ratanasthien, B.; Sititach, S. The Carboniferous flora of northeastern Thailand: Additional documentation from the Na Duang—Na Klang basin. *Rev. Paléobiol. Genève* **2009**, *28*, 315–331.
8. Fontaine, H.; Salyapongse, S.; Utha-aroon, C.; Vachard, D. Age of limestones associated with gypsum deposits in northeast and central Thailand, A first report. *CCOP Newslett.* **1997**, *21*, 6–10.
9. Holser, W.T. Catastrophic chemical events in the history of the ocean. *Nature* **1977**, *267*, 403–408. [CrossRef]
10. Claypool, G.E.; Holser, W.T.; Kaplan, I.R.; Sakai, H.; Zak, I. The age curves of sulfur and oxygen isotopes in marine sulfate and their mutual interpretation. *Chem. Geol.* **1980**, *28*, 199–260. [CrossRef]
11. Burke, W.H.; Denison, R.E.; Hetherington, E.A.; Koepnick, R.B.; Nelson, H.F.; Otto, J.B. Variation of seawater 87Sr/86Sr throughout Phanerozoic time. *Geology* **1982**, *10*, 516–519. [CrossRef]
12. Grinenko, V.A.; Krouse, H.R.; Nikanorov, A.M. Use of hydrochemical and isotopic criteria for the evaluation of the influence of technogenic sulfur on surface waters. In Proceedings of the Isotope Techniques in Water Resources Development, IAEA, Vienna, Austria, 11–15 March 1992; pp. 477–494.
13. Palmer, M.R.; Edmond, J.M. The Strontium Isotope Budget of the Modern Ocean. *Earth Planet. Sci. Lett.* **1989**, *92*, 11–26. [CrossRef]
14. Cooper, M.; Herberrt, R.; Hill, G. The structural evolution of Triassic intermontane basins in northeastern Thailand. In Proceedings of the International Symposium on Intermontane Basins: Geology & Resources, Chiang Mai, Thailand, 30 January–2 February 1989; pp. 231–242.
15. Mitchell, A. Mesozoic and Cenozoic regional tectonics and metallogenesis in mainland SE Asia. In Proceedings of the GEOSEA V, Lumpur, Malaysia, 9–13 April 1984; Geological Society of Malaysia Bulletin 20. Geological Society of Malaysia: Wilayah Persekutuan, Malaysia, 1986; pp. 221–239.
16. Metcalfe, I. Origin and assembly of south-east Asian continental terrenes. In *Gondwana and Tethys*; Audley-Charles, M.G., Hallam, A., Eds.; Geological Society: London, UK, 1988; pp. 101–118.

17. Chairangsri, C.; Hinze, C.; Machareonsap, S.; Nakornsri, N.; Silpalit, M.; Sinpool-Anunt, S. *Geological Map of Thailand 1:50,000 Exploration for Sheet Amphoe Pak Chom 5345 I, Ban Na Kho 5344 I, Ban Huai Khob 5445 IV and King Amphoe Nam Somm 5444 V*; Geol. Ib. B73: Hanover, Germany, 1990; p. 109.
18. Maruoka, T.; Koeberl, C.; Hancox, P.J.; Reimold, W.U. Sulfur geochemistry across a terrestrial Permian-Triassic boundary section in the Karoo Basin, South Africa. *Earth Planet. Sci. Lett.* **2003**, *206*, 101–117. [CrossRef]
19. Roveri, M.; Lugli, S.; Manzi, V.; Gennaria, R.; Schreiber, B.C. High-resolution strontium isotope stratigraphy of the Messinian deep Mediterranean basins: Implications for marginal to central basins correlation. *Mar. Geol.* **2014**, *349*, 113–125. [CrossRef]
20. Takahashi, T.; Hirahara, Y.; Miyazaki, T.; Vaglarov, B.S.; Chang, Q.; Kimura, J.-I.; Tatsumi, Y. Precise determination of Sr isotope ratios in igneous rock samples and application to micro-analysis of plagioclase phenocrysts. *JAMSTEC Rep. Res. Dev.* **2009**, *2009*, 59–64. [CrossRef]
21. Kuroda, J.; Hara, H.; Ueno, K.; Charoentitirat, T.; Maruoka, T.; Miyazaki, T.; Miyahigashi, A.; Lugli, S. Characterization of sulfate mineral deposits in central Thailand. *Island Arc* **2017**, *26*. [CrossRef]
22. McArthur, J.M.; Howarth, R.J.; Shields, G.A. Strontium isotope stratigraphy. In *The Geologic Timescale 2012*, 1st ed.; Gradstain, F.M., Ogg, J.G., Schmitz, M.D., Ogg, G.M., Eds.; Elsevier: New York, NY, USA, 2012; pp. 127–144, ISBN 9780444594259.
23. Kampschulte, A.; Strauss, H. The sulfur isotopic evolution of Phanerozoic seawater based on the analysis of structurally substituted sulfate in carbonates. *Chem. Geol.* **2004**, *204*, 255–286. [CrossRef]
24. Hudson, J.D. Stable isotopes and limestone lithification. *J. Geol. Soc.* **1977**, *133*, 637–660. [CrossRef]
25. Worden, R.H.; Smalley, P.C.; Fallick, A.E. Sulfur cycle in buried evaporates. *Geology* **1997**, *25*, 643–646. [CrossRef]
26. Paytan, A.; Kastner, M.; Campbell, D.; Thiemens, M.H. Sulfur isotopic composition of Cenozoic seawater sulfate. *Science* **1998**, *282*, 1459–1462. [CrossRef] [PubMed]
27. Lazar, B.; Erez, J. Carbon geochemistry of marine-derived brines: I. ^{13}C depletions due to intense photosynthesis. *Geochim. Cosmochim. Acta* **1992**, *56*, 335–345. [CrossRef]
28. Dickson, J.A.D.; Coleman, M.L. Changes in Carbon and Oxygen Isotope Composition during Limestone Diagenesis. In *Carbonate Diagenesis*; Tucker, M.E., Bathurst, R.G.C., Eds.; Blackwell Scientific Publications: London, UK, 2009; pp. 259–270, ISBN 978-1-444-30452-7.
29. Allan, J.R.L.; Matthews, R.K. Isotopic signatures associated with early meteoric diagenesis. *Sedimentology* **1982**, *29*, 797–817. [CrossRef]
30. James, N.P.; Choquette, P.W. Limestones—The sea floor diagenetic environment. In *Diagenesis*; Mcllreath, I.A., Morrow, D.W., Eds.; Geoscience Canada Reprint Series No.4; Geoscience Canada: Burnaby, BC, Canada, 1990; pp. 75–112.
31. Marshall, J.D. Climatic and oceanographic isotopic signals from the carbonate rock record and their preservation. *Geol. Mag.* **1992**, *129*, 143–160. [CrossRef]
32. Decima, A.; McKenzie, J.A.; Schreiber, B.C. The origin of evaporative limestones: An example from the Messinian of Sicily (Italy). *J. Sed. Petrol.* **1988**, *58*, 256–272. [CrossRef]
33. Bottrell, S.H.; Newton, R.J. Reconstruction of changes in global sulfur cycling from marine sulfate isotope. *Earth Sci. Rev.* **2006**, *75*, 59–83. [CrossRef]

© 2018 by the authors. Licensee MDPI, Basel, Switzerland. This article is an open access article distributed under the terms and conditions of the Creative Commons Attribution (CC BY) license (http://creativecommons.org/licenses/by/4.0/).